Available online at www.sciencedirect.com

ScienceDirect

journal homepage: www.jfda-online.com

Original Article

Design, synthesis and evaluation of DNA nanocubes as a core material protected by the alginate coating for oral administration of anti-diabetic drug

Mirza Muhammad Faran Ashraf Baig [a,b,*], Muhammad Abbas [c], Muhammad Naveed [d,e], Said Abasse Kassim [f], Ghulam Jilany Khan [g], Muhammad Sohail [i,e], Sana Ullah [c], Muhammad Hasnat [h], Komal Shah [e], Muhammad Tayyab Ansari [b]

[a] State Key Laboratory of Analytical Chemistry for Life Sciences, School of Chemistry and Chemical Engineering, Nanjing University, Nanjing, 210023, China
[b] Department of Pharmaceutical Chemistry, Faculty of Pharmacy, Bahauddin Zakariya University, Multan, 60000, Pakistan
[c] State Key Laboratory of Pharmaceutical Biotechnology, School of Life Sciences, Nanjing University, Nanjing, 210023, China
[d] Department of Clinical Pharmacology, School of Pharmacy, Nanjing Medical University, Nanjing, 211166, Jiangsu Province, PR China
[e] Faculty of Pharmacy and Alternative Medicine, The Islamia University of Bahawalpur, Bahawalpur, 63100, Pakistan
[f] Key Laboratory of Environmental Medicine Engineering, Ministry of Education, School of Public Health, Southeast University, Nanjing, China
[g] Faculty of Pharmacy, University of Central Punjab, Lahore, 54570, Pakistan
[h] Jiangsu Key Laboratory of Drug Screening, China Pharmaceutical University, Nanjing, 210009, China
[i] School of Pharmacy, Nanjing Medical University, Nanjing, 211166, Jiangsu Province, PR China

ARTICLE INFO

Article history:
Received 7 March 2019
Received in revised form
27 March 2019
Accepted 29 March 2019
Available online 23 April 2019

Keywords:
Type 2 diabetics
3D DNA nanocube

ABSTRACT

Poor control towards glycemic levels among diabetic patients may lead to severe micro/macro-vascular and neuropathic complexities. Proper functioning of alpha-beta cells of pancreases is required to attain long term glycemic control among type 2 diabetics. The recent developments to manage diabetes are focused on controlling the insulin-glucagon secretions from the pancreases. DPP-4 inhibitors class of drugs after elevating GLP-1/GIP (incretins) levels in the blood, not only raise the insulin levels but also suppress the glucagon level. Vildagliptin (VI) is a potent DPP-4 inhibitor with least adverse events compared to other DPP-4 inhibitors. We encapsulated VI into 3D nanocube that gets bind to the DNA due to secondary amine in its chemical structure. DNA-nanocube being negatively charged was incubated with the PLL to attain positive surface. Ultimately VI loaded

Abbreviations: PLL, Poly-L-lysine; 3D, 3 dimensional; VI, Vildagliptin; DPP-4, Dipeptidyl-peptidase 4; GLP-1, Glucagon-like-polypeptide 1; GIP, Gastric-inhibitory-peptide.

* *Corresponding author*. State Key Laboratory of Analytical Chemistry for Life Sciences, School of Chemistry and Chemical Engineering, Nanjing University, Xianlin Campus, Nanjing, 210023, China.
E-mail address: mirzafaran-ashraf@hotmail.com (M.M.F.A. Baig).

https://doi.org/10.1016/j.jfda.2019.03.004

Vildagliptin
Db–Db/mice
Nanospheres

nanocubes were coated with the negatively charged Na-alginate via electrostatic attraction method to get stable spherical nanospheres for oral delivery of VI. Nanospheres were evaluated physically through native PAGE analysis, DSC, TGA, dissolution testing, XRD and FTIR. We attained uniformed and spherical nanospheres with stable topology, nanoscale size precision (40–150 nm in diameter), Entrapment efficiency (up to 90%), prolonged drug release (13 ± 4 h) at basic pH, and superior oral antidiabetic effects with improved GLP1 and glycemic levels. The formulated nanospheres attained size uniformity and better therapeutic outcomes in terms of reduced adverse events and better control of glycemic levels than previously reported methods with decreased dosage frequency tested in Db/Db mice.

1. Introduction

Last decade is evidence of increased malignant cases of various types of cancers that are resistant towards treatment affecting patients of all ages [1,2]. However, the disease turning out to be more devastating is Type 2 diabetes even spreading among the young people belonging to different age groups [3]. The reason is either increasing stress or hardships in life or increased leisure due to over eating or spending time on watching TV or playing games and decreased sleep habits [3]. Type 2 diabetes is a complex metabolic disease primarily diagnosed through consistent elevations in the glycemic levels of diabetes mellitus patients [4]. These sustained elevations of the patient glycemic status further cause polyuria, polydipsia, and increased osmolality of the blood and even disturbs all the processes being occurred in the body [5]. On the long run if it remains uncontrolled may lead to neuropathy, nephropathy, retinopathy, fatty liver and cardio-vascular complications with decreased HDL levels and increased LDL and VLDL levels in the blood [4]. The tissues of the body and the cells might attenuate self-ability to respond to the insulin and acquire resistance. However, in some cases, it has been found that excessive glucagon secretion from the pancreatic alpha cells is also the main cause of raising the blood glucose level due to its action on the liver to cause glucogenesis, gluconeogenesis as well as glycogenolysis and decreasing the glycogenesis [5]. It also has secondary effects of decreasing proteolysis and lipolysis [4]. Furthermore, it causes feedback inhibition of the secretion of the insulin from pancreatic beta-cells [5]. So, glucagon, by all means, causes elevations in the blood glucose levels. GLP-1 is the hormone secreted naturally from the k-cells of the intestine during food digestion and glucose absorption that causes direct feedback inhibition of the glucagon secreted from the pancreatic alpha-cells [5]. It further combine its effect with the other incretin hormone known as GIP to act on the pancreatic beta-cells to secrete insulin [6]. So these incretin hormones (GLP-1 and GIP) promote postprandial insulin secretions and suppression of the glucagon release [5]. Sometimes chronic diabetic patients taking sulphonyl-ureas or other secretagogues develop either insulin resistance or beta cells exhaustion. It is due to the continuous action of these drugs on the beta cells to synthesize and releases insulin continuously with or without food intake [3]. That also increases the risks of hypoglycemia in acute type 2 diabetic patients due to excessive secretions of the insulin that may lead towards either beta cells exhaustion or beta cells depletion [7]. However oral GLP-1 boosting therapies specially the DPP-4 inhibitors after elevating the GLP-1 and GIP level in the blood, not only improves post prandial glycemic level in a glucose dependent manner but also on a long term have been found to cause beta cells neo-genesis and repair of the damaged part of the islets of Langerhans in the pancreases of diabetic patients [8].

Nanoparticles based on DNA materials are gaining significance during the past few years [9]. DNA based materials can be designed in any shape with nanoscale size by the simple addition of the oligonucleotides with a specific sequence in equimolar concentrations that may combine to each other according to the Watson/Crick complementarity with the ease of fabrication [10,11]. Many reports demonstrated the materials based on DNA nanotechnology with the specific features suitable for various potential advancements towards biosensing, delivering APIs to the target-sites and in nanoelectronics [12–14]. In this report, we have designed DNA-nanocube by circular DNA nanotechnology. After circularization of the two 84-NT strands followed by the self-assembly with the 4 staple strands resulting in the DNA-nanocube [15]. The sequences of the circular templates and the staple strands have been mentioned in Table 1. The resultant DNA-nanocubes were loaded with the VI and underwent charge inversion using PLL treatment to attain the positive charge [16]. After that Na-alginate coating was applied on the VI loaded DNA-nanocubes to further solidify by calcification technique to form gastric resistant, polymer-protected nanospheres [17]. For evaluating the nanospheres for oral enteric sustained release delivery of VI, we used Db–Db mice with similar metabolic status as that of patients suffering from diabetes [18,19].

Sodium Alginate is found in nature as a polysaccharide copolymer having β(1–4)linkage between the D-mannuronic-acid and α-L-guluronic-acid monomers, primarily processed from either brown-seaweed or brown-algae found in both marine as well as fresh cold-water ponds [20,21]. Vigorous stirring is required to solubilize it in cold water. To thicken it into gel-like-material or to make solid nanoparticles, calcination is performed using $CaCl_2$ without requirement of high temperature [22]. This property of Na-alginate makes it

Table 1 – Sequences of oligonucleotides used in this study.

Name of DNA oligonucleotides	Sequences (5′ to 3′)
Scaffold strand 1	GACCTGACTGGAGTCGGATTCCATATGTTCATTCGCTCATCT GCTAATGTCATCGGTGAATCGTTAGGCCTGAGAATTCGGATA
Scaffold strand 2	TAGCGGTCATGAGCTGCCGGATATTGCAATGGACTGGATCTAAG TCTGAACCTTAGTTGCAAGACGGTACCTGAGAATGATACG
Splint 1	CAGTCAGGTCTATCCGAATT
Splint 2	ATGACCGCTACGTATCATTC
Staple 1	GCTAGGCATGACCGCTACGTATCATTCCTGATC
Staple 2	GGAGCCATGAACATATGGAATCCGACTACATTAGTGACCAATCGC ATTCCTAGC
Staple 3	AATGCGATTGGTCACTAATGTCCAGTCAGGTCTATCCGAATTTCTA TGGTAGCACTAGCCTAGAACTCA
Staple 4	AATGAGCCATTGCAATATCCGGCAGCT
Staple 5	CGTTATAAGCTTGTCTAGACTCAAACGCTCATT
Staple 6	ACGATCAAGTCTGATGACTACAGGTTCAGACTTAGATCCAGTCGTTT GAGTCTAGACAAGCTTATAACG
Staple 7	CTGACCATGACATTAGCAGATGAGCGAGGCTCC
Staple 8	GACTGGCATAGGAGCCTATCAAGACAGATCAACGTTCTGCCATGGACT
Staple 9	CATAGACTCAGGCCTAACGATTCACCGCGAGGT
Staple 10	GATCAGTGAGTTCTAGGCTAGAGCTACTCTATG

suitable to add with the PLL-DNA-nanostructures at room temperature to electrostatically combine with the DNA. After further addition of di-valent ions (calcium), which might not only stabilize the DNA nano-architects but also cause the gelation of alginate forming a solid insoluble coat around the PLL-DNA nano-architects into solid nanospheres [22]. These calcified nanospheres are not digested in the stomach bypassing it effectively to reach the intestine that is the target site for our study where GLP-1 is released into the blood upon glucose absorption [17]. But as intestinal membranes and other biological membranes in the body also secrete DPP-4 enzyme in to the blood, which may inhibit the released GLP-1 and GIP [8]. Therefore, effective inhibition of DPP-4 enzyme in the intestinal membrane with higher efficiency is a desirable element [7].

According to the previously reported data, Vildagliptin (VI) has established itself as a potential and selective DPP-4 inhibitor. Therefore it was found to be less associated with the occurrence of pancreatitis, pancreatic-cancer, prostatitis and angioedema [8,23,24]. Hence, safety profile of the VI has been established to be superior to the other DPP-4 inhibitors being marketed such as Sitagliptin, Saxagliptin, Alogliptin and Linagliptin [25]. It escapes from the metabolism by liver microsomal-enzyme system (Cyp-450). However it is metabolized by non-microsomal hydrolases of the liver. This unique parameter makes it superior than the Sitagliptin in terms of drug to drug interactions with other drugs being metabolized by Cyp-450 system [26]. As diabetic patient may also develop cardiovascular or hyperlipidemic complications. Therefore, needs a combination of various medications simultaneously. Most of the drugs used as antihypertensive drugs such as ACE-inhibitors as well as cardiotonic drugs such as digoxin and digitoxin and anti-platelet drugs such as warfarin and the anti-hyperlipidemic drugs such as statins are metabolized by CYP-450 system. For such types of complex patients, unlike Sitagliptin, VI have minimum drug to drug interactions [26]. Unlike Sitagliptin, It also does not require to adjust the dose in patients with renal-impairment and effectively raise the blood incretins (GLP-1 & GIP) level released by the k-cells of the intestine boosting the insulin release from the β-cells with wrecked release of glucagon from the α-cells [25]. VI after potent DPP-4 enzyme inhibition, stop the sabotaging these peptide hormones, and raising its serum levels [7]. However half-life of VI is just 2.5–2.8 h. Therefore, we have developed a novel formulation to shatter DPP-4 enzyme more effectively by enteric delivery of VI with slow and prolonged properties. Due to use of VI loaded DNA-nanocube as scaffold coated by alginate polymer, the resulting nanospheres got small size and uniformity among the nanoparticles. These particles may bypass the stomach to reach the target-site (intestine) where DPP-4 enzyme is released from the membrane-cells. Some of the tiny nanospheres (300 nm–2 μm diameter) might also be absorbed through the intestine for further prolonging the DPP-4 inhibition.

2. Materials and methods

2.1. *Materials*

DNA oligo-strands (Sangon'Biotechnology Shanghai'China), Db–Db-mouse (Animal'modeling/institute' China'Pharmaceutical-University Nanjing'China). Alginate and PLL (Evonik'industries Karachi'Pakistan), XRD-instrument (Bruker'USA), FTIR-instrument (Thermo'Fischer/Scientific'USA)T4-DNA'ligase (Sangon'Biotechnology Shanghai'China), Exonuclease 1 (Sangon'Biotechnology Shanghai'China), UV-spectroscopy/instrument (Thermo'Fischer/Scientific'USA), deionized-formamide (Sangon'Biotechnology Shanghai'China), n-butanol/ethanol (Beijing'Chemical Company Beijing'China), Fast-Scan'AFM/instrument-Bruker'USA, polyacrylamide'bisacryl 30%'solution (Sangon'Biotechnology Shanghai'China), ammonium-persulfate (Sangon'Biotechnology Shanghai'China), TEMED (Shanghai'Chemical Company

Shanghai'China), Vildagliptin (received from High-Q'Pharma Karachi'Pakistan). Gel-analysis-instrument (Thermo'Fischer/Scientific'USA), PAGE'electrophoresis instrument (Bio'Rad-California'USA), Nanodrop'1000 and 2000c (Thermo'Fischer Scientific'USA).

2.2. Synthesis of DNA-nanocubes

After ordering DNA-oligostrands from Sangon-Biotechnology-company, Shanghai, were undergone purification process using PAGE technique. Purified strands were undergone UV analysis with ss-DNA-protocol for concentration-measurement using Nanodrop-1000. The purified strands were self-assembled into designed DNA nano-cubes [27]. We have mentioned the sequence of the above strands in Table 1. The illustration of the DNA nano-cube structure has been drawn in Fig. 1A. The synthesis of the DNA-nanocube is explained in Fig. 1B and Fig. 1C.

2.3. Detailed methodology

The detailed methodology has been mentioned in supporting information.

2.4. Administration of nanoparticles

Nanoparticles were administered orally by mixing the suspension of the nanoparticles with the water drank by the mice. 30 μL aqueous suspension of the nanoparticles as one dose with 30 μg drug for the mice of 25–28 g weight was administered orally, immediately after taking food, as GLP1 secretion from the intestine occurs during glucose absorption from the intestine after food intake. The control group also received 30 μg of free drug post prandial. DNA scaffold nanoparticles are biocompatible and less toxic than the previously reported materials [28,29].

2.5. Statistical-evaluation

Origin'Pro-9.1 was used to illustrate and analyze the data. Every experiment was undergone for at least three individual repetitions to ensure reproducibility to calculate average values and to get SD'values. Anova & T tests were estimated between the groups A&B to find confidence interval and significance level which was according to the following criteria. $P < 0.02$ to $p < 0.002$ (*, $p < 0.02$; **, $p < 0.01$; ***$p < 0.002$) [30].

2.6. Animal ethics

Animal ethics were strictly considered during all the experiments involving Db/Db'mice. As approved and mentioned by the Ministry of Health'China and the China'Pharmaceutical University'China.

3. Results

3.1. Loading encapsulation-efficiency (E.E%) of VI

The calculations employed in this study to calculate the E.E % for DNAnano-cube and VI has been given in the materials and methods section above as equations 1&2. After using 0.34–0.36 μg of DNA and 0.35 μg of VI to prepare one batch of the nanospheres, it was centrifuged to take a sample of the supernatant to evaluate the amount of unencapsulated DNA (0.024–0.026 μg). For instance, The E.E % measurement of the DNAnano-cube for the NS6 formu-

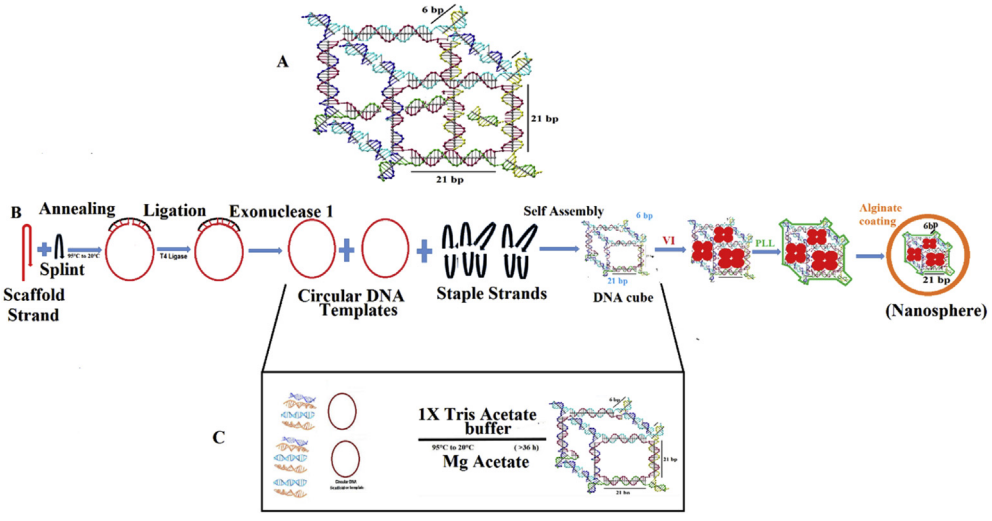

Fig. 1 – Mechanistic approach to synthesize the DNA nano-cube and the alginate-PLL-DNA-VI nanospheres: A) DNA nano-cube was synthesized to act as a skeleton for the VI loading and PLL-alginate coating to obtain the stable nanospheres. B) The illustration of the main steps to make the designed nanosphere C) Detail of the key steps to synthesize the DNA nano-cube made from two circular/template strands self-assembled with the ten staple strands (25 μM each).

Table 2 – Batches of Nanoparticles with different polymer concentrations.

B#	Alginate (%)	PLL %	E.E% DNA (Loading)	E.E% VI (Loading)
NS1	0.01	0.02	79.28 ± 5.54%	70.11 ± 6.48%
NS2	0.02	0.02	82.28 ± 3.21%	74.65 ± 3.85%
NS3	0.03	0.02	84.75 ± 4.16%	76.43 ± 1.63%
NS4	0.04	0.02	85.38 ± 3.91%	78.66 ± 2.99%
NS5	0.05	0.02	87.74 ± 2.88%	79.88 ± 3.78%
NS6	0.06	0.02	89.28 ± 3.73%	83.35 ± 5.61%

lation (PLL'0.03% & alginate 0.06%) was 89.28 ± 3.73%. Whereas, the E.E% for the VI for the above formulation was 83.35 ± 5.61 (Table 2).

3.2. *AFM analysis*

The surface of the alginate-PLL-DNA-VI nanospheres was round, smooth and uniform with the size range between 5 and 250 nm in diameter depending on the degree of mechanical stirring of the shaking device as well as the concentration of alginate polymer. More the concentration of the alginate, larger was the diameter of the synthesized nanospheres [20]. The AFM image of the nanospheres of the NS1 batch has been shown in Fig. 2A.

3.3. In vitro *release experiment of VI from alginate-PLL-DNA-VI nanospheres*

For the dissolution testing at acidic pH, simulated'gastric'solution was used. We found that the alginate coat over nanospheres remained intact even after 13–17 h without significant release of VI due to pH'dependent-swelling and effective entrapment within the core made up of DNAnano-cube. However nanospheres showed time'dependent swelling at basic'pH with first-order release during one to 6 h interval followed by zero-order release up to 15 h. The release profile of VI of different formulations (NS1 to NS6) has been shown in Fig. 2B.

3.4. *Evaluation of mechanical strength of the nanospheres*

Native Page experiment was done, and illustrated in Fig. 2C. Lane 4 of the gel is representing the band of PLL-DNA. After combining positively charged PLL to the negatively charged DNA nano-cubes through electrostatic interactions, the resulting PLL-DNAnano-cube lost its electrophoretic mobility and gave a single band at the top of the gel without moving down the gel. However after coating of the negatively charged alginate over the PLL-DNA, the electrophoretic mobility of the alginate-PLL-DNA-VI nanospheres was increased due to the negative surface charge on the nanospheres. The single band in the lane 5 indicates the stable and mechanically compact

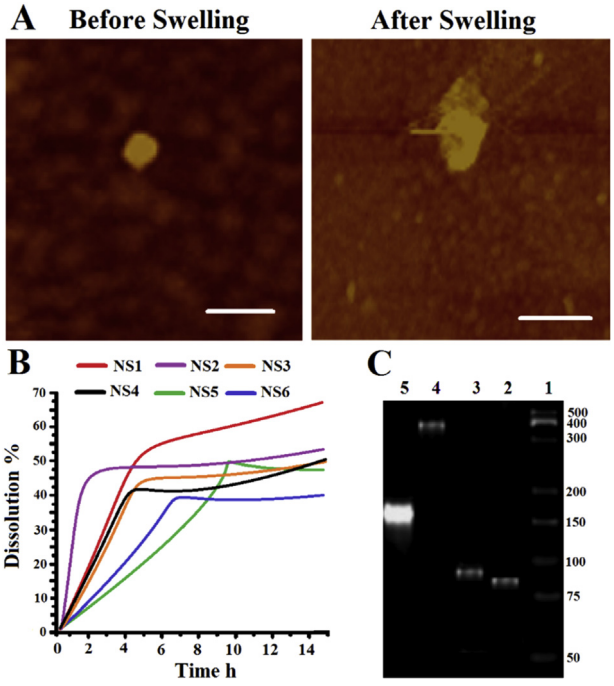

Fig. 2 – Characterization of the alginate-PLL-DNA-VI nanospheres: A) AFM imaging of the NS3 nanosphere confirming the round and uniform shape with the size of 50–100 nm (diameter) Scale bar = 200 nm. B) Dissolution study in the basic buffer (pH 8.5). Blue curve representing NS6 formulation shows the slowest release in sustained manner due to the higher alginate concentration and resistance towards gelling or swelling. C) The linear and circularized scaffolds (84-NT each) travelled down the gel (Lane 2 and 3), whereas PLL-DNA could not travel down the gel due to positive coating of PLL over DNA. However nanospheres of the NS6 batch (Lane 5), in spite of the large size showed some electrophoretic mobility due to the negative surface charge on the nanospheres after alginate coating. It gave one sharp band showing strength and integrity of nanospheres.

nature of the nanospheres giving a sharp band. However due to very large molecular size of the alginate coated VI loaded, PLL-DNAnano-cubes, nanospheres could not travel down the gel to the longer distance.

3.5. *Physical-testing for the assessment of the formulation*

3.5.1. *Attenuated total reflection (ATR)-FTIR*

FTIR spectra of the alginate polymer used in this work exhibit sharp signal at 1518 cm^{-1}. However this characteristic peak of the alginate is shifted to 1523 cm^{-1} in the nanospheres (with or without VI loading) due to surface coating. Whereas FTIR

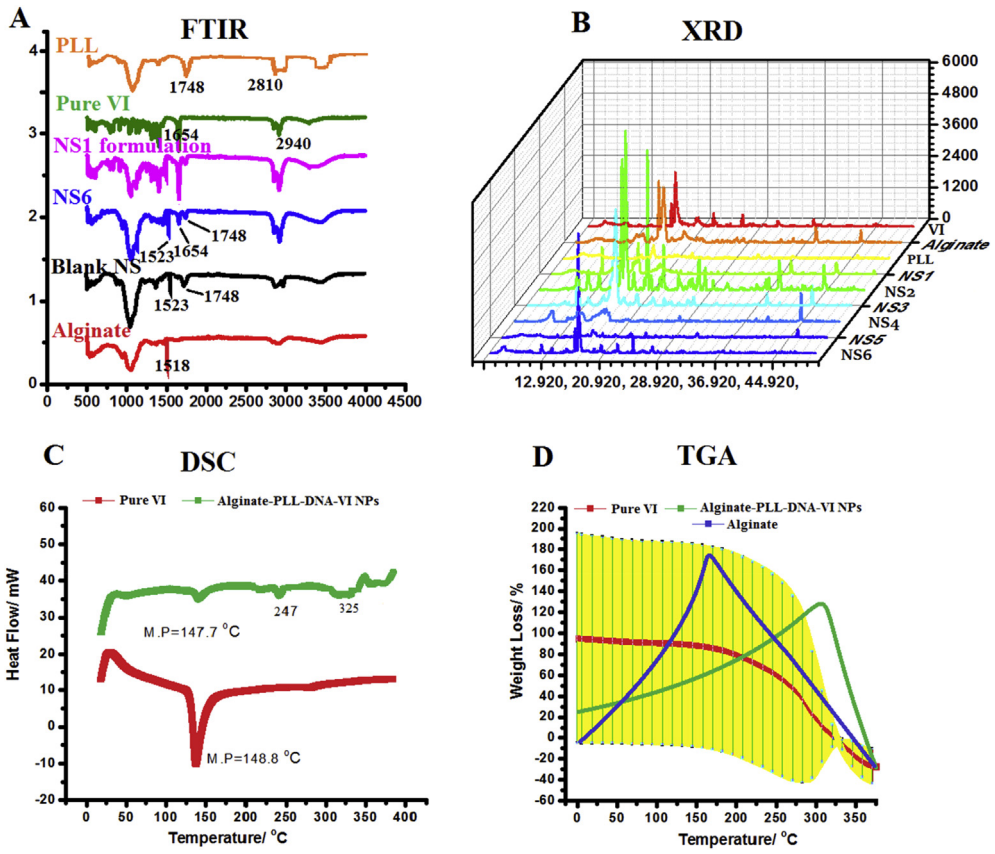

Fig. 3 – Physical characterization of the alginate-PLL-DNA-VI nanospheres: A) FTIR of the pure alginate (bottom spectrum) exhibited sharp-peak at 1518 cm^{-1} that was shifted to 1523 cm^{-1} in the formulation. FTIR of PLL (top spectra) showed characteristic peak at 1748 cm^{-1} whose intensity became diminished in the formulation. VI characteristic peak at 1654 cm^{-1} also got feeble in the formulation (Pink and Blue). VI peak was absent in the blank formulations (black spectra) confirmed the compatibility of VI with excipients. B) XRD spectra clearly depicted the morphology change of the crystalline status of VI and excipients in the nanospheres. C) DSC of the nanospheres (NS6 batch) showed some shifting of the melting points due to the encapsulation and physical embedding effects. D) TGA (Thermo/gravimetric-analysis) showed changes in the LOH (loss of hydration) due to the encapsulation and physical embedding effects.

spectra of PLL exhibits characteristic peak at 1748 cm^{-1} that also persists in the nanosphere formulation. The characteristic peak of VI is at 1654 cm^{-1}. This peak of VI was present only in the VI loaded nanospheres and absent in the blank nanospheres without VI loading [22]. The above findings confirm the compatibility of VI with other excipients in the nanospheres (Fig. 3A).

3.5.2. *XRay-diffraction (XRD)*

We observed different pattern of peaks in case of nanospheres as compared to pure excipients. After dispersing the excipients physically into nanospheres undergo recrystallization causing changes in the crystalline behavior of the nanospheres, successful physical dispersion as well as VI encapsulation inside the nanosphere matrix. Fig. 3B shows that XRD of the pure VI has different pattern of crystalline behavior as compared to thr formulated nanospheres. Pure-VI shows peaks at 6.907°, 9.826°, 10.653°, 11.565°, 13.954°, 14.478°, 15.857°, 17.766°, 18.438°, 19.639°, 20.756°, 20.295°, 22.638°, 25.387°, 26.261°, 26.407°, 29.674° and 30.169°. We observed that, XRD of the VI loaded nanospheres was different from that of pure excipients (Fig. 3B) [20].

3.5.3. *Differential'scanning-calorimeter analysis for melting-points (M.P.)*

The melting-point (M.P.) of pure-VI is 148.8 °C. The DSC-thermogram of the NS6 batch of the nanospheres showed a shift of the M.P of the VI to 147.7 °C. It happened due to the physical dispersion of the VI within the nanosphere matrix. The melting point peak for the PLL was shifted from 250 °C to 247 °C in the NS6 nanosphere formulation. The peak for alginate remained unchanged at 350 °C, indicating compact surface coating by alginate (Fig. 3C) [20].

3.5.4. *Thermal gravimetric analysis (TGA)*

The weight loss (%) of pure VI decreased with the heating process. However in case of alginate, it increased with the increase in temperature, due to the gelling property of the polymer and the incorporation of water. However later it decreased rapidly with the quick loss of water due to drying effect. The nanospheres having alginate coating also showed the similar pattern. First increase in weight loss followed by the sharp decrease to the zero level (Fig. 3D).

3.6. In vivo *testing of the alginate-PLL-DNA-VI nanospheres*

In vivo experiments on the DB-DB-mice confirmed the safety of the nanospheres for 21 weeks [7]. The positive control as well as the alginate-PLL-DNA-VI nanospheres did not damage the histology of pancreatic tissue shown in Fig. 4A. Alginate-PLL-DNA-VI nanospheres were administered orally to the group A of DB/DB mice simultaneously with the diet for 21 weeks. Mice for monitored at scheduled time postprandial for taking blood samples to analyze the GLP1 and glycemic levels. Upon completion of the treatment duration, the sacrificed mice were undergone histo-pathological examination to know the status of the pancreatic endocrine portion [4,18]. We found that the endocrine portions of the pancreas of the mice from both of the groups ((treatment & control) showed normal status [25]. We did not found any event of tumor/metastasis, inflammation/fibrosis and necrosis (Fig. 4 A). Herein, after administration of the alginate-PLL-DNA-VI nanospheres to the group A mice, it bypassed the stomach effectively and reached the intestine along with the food after 1.5 h where it released VI slowly in a prolonged way.

According to the plasma drug concentration evaluation through LC-Mass, VI release after the first hour was rapid and was found to be 2.75 ng/μl. This quick release of VI might be due to the gelling and swelling of alginate coat after reaching intestine and following first order diffusion effects of VI from the core to the surface of nanospheres. With the further swelling and diffusion effects the release of VI was further increased and plasma drug level was increased to 4.57 ng/μl, 5.65 ng/μl, 6.76 ng/μl and 7.39 ng/μl after each hour increment up to 5 h following first-order-diffusion/kinetics. Whereas, the group B of mice that received VI-solution, the plasma VI concentration evaluated after first hour was 11.97 ng/μl.

It was because free VI-solution had a quick absorption to the blood. Conversely, after the second hour, plasma VI-level began to be decreased to 10.25 ng/μl. It further decreased to 8.67 ng/μl, 6.65 ng/μl and 5.36 ng/μl after each hour up to 5 h. It was interesting to observe that GLP1 level in the plasma was independent of the VI concentration in the blood owing to the dependency of the release of the GLP1 on the food intake and the glucose absorption through the intestine.

As release characteristics of the VI was dependent upon the nanospheres properties, formulations parameters and the kinetics of the swelling and diffusion of the drug to the surface, we found that administration of these nanospheres resulted in the improved GLP1 and blood glucose status in group A (treatment) verses group B (positive control). VI blocked the DPP-4 more effectively in group A after the postprandial release of GLP1 improving the glycemic level not only after the meal but for all day long due to the sustained release kinetics of the nanospheres [25,30].

The GLP-1 and the blood glucose level measured on hourly basis postprandial after 12 weeks of treatment compared to the positive control has been shown in Fig. 4B and C. The maximum level of the GLP1 observed for the group A (treatment-group) which received alginate/PLL-DNA-VI nanospheres was recorded to be 0.12—0.16 pg/μL at 3 h interval postprandial after the administration of the nanospheres with the food. Even after 4 h, the GLP1 level was still significantly high up to 0.088—0.098 pg/μL. Conversely, control group which received VI solution as positive control that caused elevation in the GLP-1 level at 3 h interval to reach the maximum level of 0.055—0.065 pg/μL but did not maintain GLP-1 level to the significant level after 5 h which decreased significantly to the level of 0.022—0.035 pg/μL. So alginate-PLL-DNA-VI was significant in improving the GLP1 as well as glycemic levels in a sustained manner compared to control group (Fig. 4) [31].

4. Discussions

The integrity of the nanospheres confirmed through the Page native Gel shown in Fig. 2C confirmed the strength and the stability of the formulated nanospheres. PLL being positively charged had a stable coating over the DNAnano-cubes. Alginate being negatively charged polymer had stable coating over the PLL-DNA due to the electrostatic interactions which made nanospheres to have mechanical strength and resistant to the stomach acidity towards protein and DNA breakdown. Mechanical strength of the alginate-PLL-DNA-VI nanospheres was evaluated through gel electrophoresis by examining changings in the electrophoretic mobility of the nanospheres and attainment of single band. Loading'Encapsulation-efficiency (E.E%) of VI was dependent primarily on the variations of the concentration ratios between the alginate: PLL: DNA: VI. If DNAnano-cube & VI concentrations was kept constant then increasing the alginate and PLL concentrations resulted into enhancement of the E.E%. NS6 formulation containing more alginate concentration was regarded to be the most stable formulation that showed slowest release of VI shown in Fig. 2B in-spite of the maximum loading/E.E% given in Table 2 [31]. The potent inhibition of DPP-4 by VI has been shown below in Fig. 5.

Being acidic polymer, alginate is a gastro-resistant polymer at acidic pH of the stomach that makes it resistant to swell in the stomach and may lead it to the intestine along with the food after 1 h where it got swelled and diffused out VI and DNA in a sustained/prolonged manner.

The dissolution-test of the alginate-PLL-DNA-VI nanospheres was performed at two different pH, i.e., pH'1.2 (HCl buffer) and pH'8.55 (TBE'buffer). The formulations, NS1 to NS6, with the increase in alginate proportions, the VI as well as the DNA (in spite of the increased E.E% given in Table 2), the release was significantly reduced. It was due to the increased compactness and strength of the nanospheres with the increase in the alginate concentrations with decreased ability to swell and diffuse DNA and VI out Fig. 2 B, [16,31].

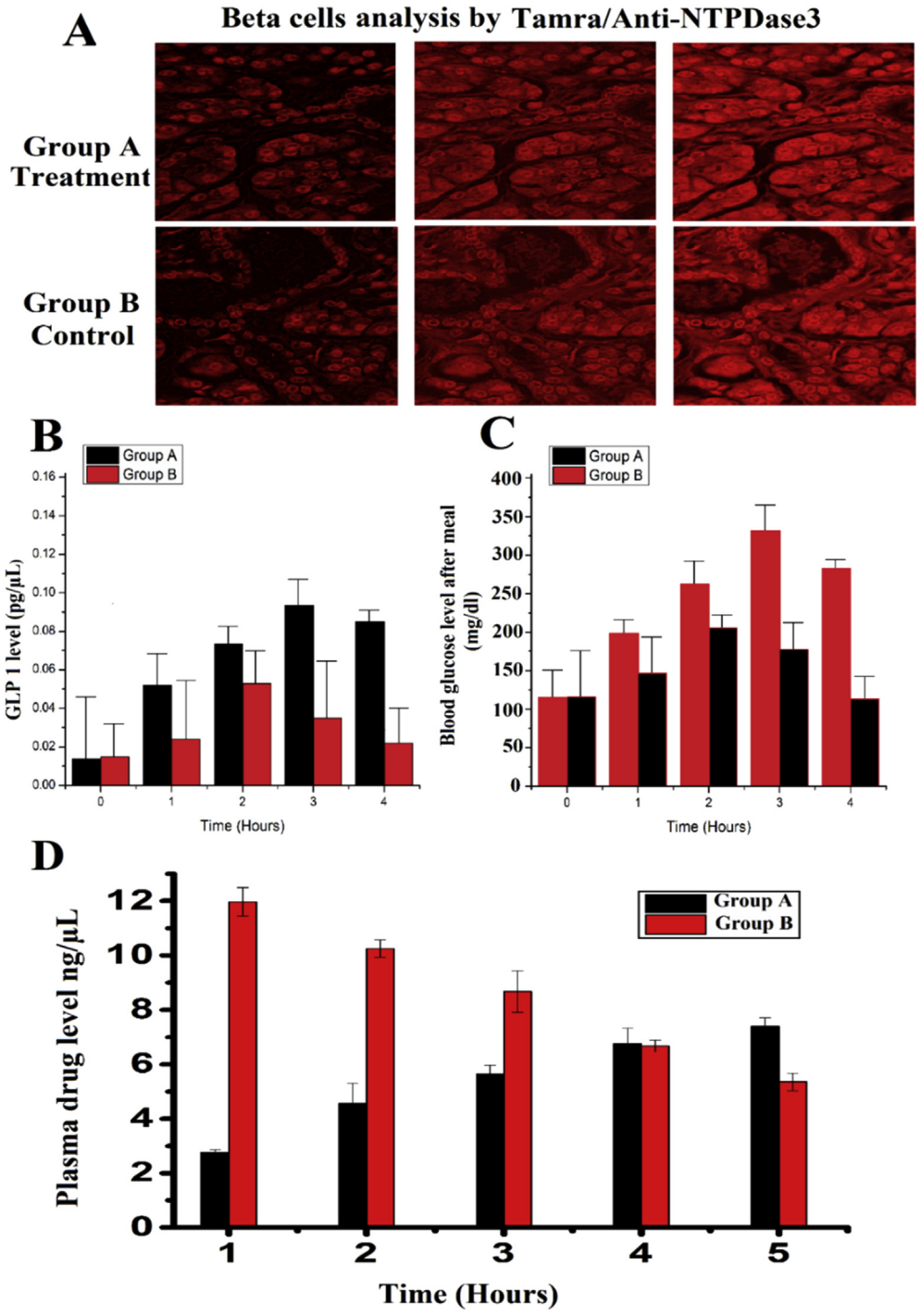

Fig. 4 – Animal experiments of five months therapy with the orally administered alginate-PLL-DNA-VI nanospheres: A) The prolonged release nanospheres had no damage to the endocrine portion of the pancrease after 5 months compared to the administration of the free VI solution. B) GLP1 elevation was higher in group A mice receiving alginate-PLL-DNA-VI nanospheres for prolonged time compared to the group B mice receiving free-VI solution. C) Glycemic status was improved in a sustained manner among group A mice receiving alginate-PLL-DNA-VI nanospheres as that of group B mice. D) Plasma level of VI with time.

AFM imaging was used to visualize the compactness of the alginate coating over the nanospheres. AFM images of the alginate-PLL-DNA-VI nanospheres of batch NS3 shown in Fig. 2A highlighted the spherical and uniform shape of the nanospheres. FTIR spectra of PLL exhibits a characteristic peak at 1748 cm^{-1} that also persists in the nanosphere formulation. Whereas FTIR spectra of the alginate polymer used in this work exhibit sharp signal at 1518 cm^{-1}. However, this characteristic peak of the alginate is shifted to 1523 cm^{-1} in the nanospheres (with or without VI loading) due to surface

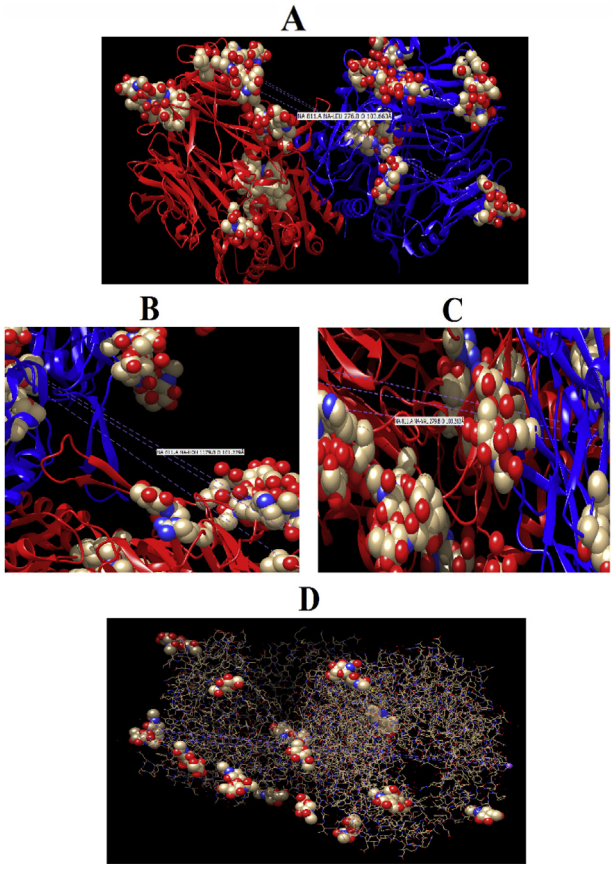

Fig. 5 – Potent inhibition of DPP-4 by VI. A&D) The DPP-4 offers 20 different sites on both of its alpha as well as beta subunits to bind with the VI. B&C) Dpp-4 further exhibit the formation of self-linkages connecting two opposite ends of the alpha and beta subunits making three parallel bonds with the length of 101.229 °A to 103.669 °A. The 811th amino acid on the alpha subunit combines with the amino acids at 276, 279 or 1179 positions of the beta chain. The simulations were carried out after downloading the 6b1e.pdb file from the protein-data/bank.

coating. The characteristic peak of VI at 1654 cm^{-1} was present only in the VI loaded nanospheres and absent in the blank nanospheres without VI loading [22].

The results for the GLP1 and glycemic level included in the Fig. 4 B and C were tested using NS6 formulation that maintained DPP-4 inhibition and maintained glycemic levels up to 24 h effectively compared to the VI-solution. As $t_{1/2}$ of the VI was quite short (2.8 h) so positive control without the sustained release of VI could not inhibit the DPP-4 enzyme effectively for the prolonged time. Infact, the release of GLP-1 from intestinal k-cells was according to the amount of glucose absorbed. So inhibition of the degradation of the GLP-1 by DPP-4 did not cause hypoglycemia. However, it resolved the hyperglycemia in an effective way in a glucose-dependent manner. Whereas secretagogues such as glinides (repaglinide) and SUs (glibenclamide) had a direct action on the beta-cells to secrete insulin whether food is taken or not in a glucose-independent way with the chances of hypoglycemia if food intake was not sufficient, and might cause beta-cells exhaustion on long term treatment. In addition to hypoglycemia, the chances of pancreatitis or pancreatic cancer were not frequently reported in the case of VI as compared to sitagliptin [26]. Liver nonmicrosomal/hydrolases take part in the metabolism of VI so there were lesser chances of interactions with the other drug in case of VI compared to the sitagliptin that is metabolized by the microsomal Cyt-P450 isoforms [26]. Release characteristics of the VI were dependent upon the nanospheres properties, formulations parameters and the kinetics of the swelling and diffusion of the drug to the surface, we found that administration of these nanospheres resulted in the improved GLP1 and blood glucose status in the group A (treatment) verses group B (positive control). VI blocked the DPP-4 more effectively in group A after the postprandial release of GLP1 improving the glycemic level not only after a meal but for all day long due to the sustained release kinetics of the nanospheres [25,30].

5. Conclusion

Alginate is a cellulosic-polymers already proven to be biocompatible, suitable for formulating prolonged-release dosage forms. Herein we have reported a novel strategy to synthesize nanospheres with better size uniformity with the VI loaded DNA core coated with the alginate-PLL due to electrostatic interactions and were evaluated for the efficiency and safety for the purpose of oral delivery of VI. We further believe, due to size uniformity and nanoscale-size of the nanospheres these nanospheres can further be evaluated for systemic delivery of some problematic drugs in complex disease conditions.

Conflicts of interest

None declared.

Appendix A. Supplementary data

Supplementary data to this article can be found online at https://doi.org/10.1016/j.jfda.2019.03.004.

REFERENCES

[1] Khan GJ, Rizwan M, Abbas M, Naveed M, Boyang Y, Naeem MA, et al. Pharmacological effects and potential therapeutic targets of DT-13. Biomed Pharmacother 2018;97:255–63. https://doi.org/10.1016/j.biopha.2017.10.101.

[2] Abbas M, Ahmed A, Khan GJ, Baig MMFA, Naveed M, Mikrani R, et al. Clinical evaluation of carcinoembryonic and carbohydrate antigens as cancer biomarkers to monitor palliative chemotherapy in advanced stage gastric cancer. Curr Probl Cancer 2019;43:5–17. https://doi.org/10.1016/j.currproblcancer.2018.08.003.

[3] Chatterjee S, Khunti K, Davies MJ. Type 2 diabetes. Lancet 2017;389:2239–51. https://doi.org/10.1016/S0140-6736(17)30058-2.

[4] Lin Y, Sun Z. Current views on type 2 diabetes. J Endocrinol 2010;204:1–11. https://doi.org/10.1677/JOE-09-0260.
[5] Olokoba AB, Obateru OA, Olokoba LB. Type 2 diabetes mellitus: a review of current trends. Oman Med J 2012;27:269–73. https://doi.org/10.5001/omj.2012.68.
[6] Lovshin JA, Drucker DJ. Incretin-based therapies for type 2 diabetes mellitus. Nat Rev Endocrinol 2009;5:262–9. https://doi.org/10.1038/nrendo.2009.48.
[7] Drucker DJ, Nauck MA. The incretin system: glucagon-like peptide-1 receptor agonists and dipeptidyl peptidase-4 inhibitors in type 2 diabetes. Lancet 2006;368:1696–705. https://doi.org/10.1016/S0140-6736(06)69705-5.
[8] Toft-Nielsen MB, Damholt MB, Madsbad S, Hilsted LM, Hughes TE, Michelsen BK, et al. Determinants of the impaired secretion of glucagon-like peptide-1 in type 2 diabetic patients. J Clin Endocrinol Metab 2001;86:3717–23. https://doi.org/10.1210/jcem.86.8.7750.
[9] Endo M, Yang Y, Sugiyama H. DNA origami technology for biomaterials applications. Biomater Sci 2013;1:347–60. https://doi.org/10.1039/c2bm00154c.
[10] Han D, Pal S, Nangreave J, Deng Z, Liu Y, Yan H. DNA origami with complex curvatures in three-dimensional space. Science 2011;332:342–6. https://doi.org/10.1126/science.1202998.
[11] Hong F, Zhang F, Liu Y, Yan H. DNA origami: scaffolds for creating higher order structures. Chem Rev 2017;117:12584–640. https://doi.org/10.1021/acs.chemrev.6b00825.
[12] Baig MMFA, Khan S, Naeem MA, Khan GJ, Ansari MT. Vildagliptin loaded triangular DNA nanospheres coated with eudragit for oral delivery and better glycemic control in type 2 diabetes mellitus. Biomed Pharmacother 2018;97:1250–8. https://doi.org/10.1016/j.biopha.2017.11.059.
[13] Keren K, Berman RS, Buchstab E, Sivan U, Braun E. DNA-templated carbon nanotube field-effect transistor. Science 2003;302:1380–2. https://doi.org/10.1126/science.1091022.
[14] Schmied JJ, Raab M, Forthmann C, Pibiri E, Wünsch B, Dammeyer T, et al. DNA origami-based standards for quantitative fluorescence microscopy. Nat Protoc 2014;9:1367–91. https://doi.org/10.1038/nprot.2014.079.
[15] Ali M, Baig MMFA, Xiao S-J, Wang M, Afshan N. DNA nanotubes assembled from tensegrity triangle tiles with circular DNA scaffolds. Nanoscale 2017;9:17181–5. https://doi.org/10.1039/c7nr04869f.
[16] Mann A, Richa R, Ganguli M. DNA condensation by poly-l-lysine at the single molecule level: role of DNA concentration and polymer length. J Control Release 2008;125:252–62. https://doi.org/10.1016/j.jconrel.2007.10.019.
[17] Marañón I, Marzo F, Ibáñez FC, Villarán M del C, Chávarri M, Ares R. Microencapsulation of a probiotic and prebiotic in alginate-chitosan capsules improves survival in simulated gastro-intestinal conditions. Int J Food Microbiol 2010;142:185–9. https://doi.org/10.1016/j.ijfoodmicro.2010.06.022.
[18] O'brien PD, Sakowski SA, Feldman EL. Mouse models of diabetic neuropathy. ILAR J 2014;54:259–72. https://doi.org/10.1093/ilar/ilt052.
[19] Naveed M, Han L, Hasnat M, Baig MMFA, Wang W, Mikrani R, et al. Suppression of TGP on myocardial remodeling by regulating the NF-κB pathway. Biomed Pharmacother 2018;108:1460–8. https://doi.org/10.1016/j.biopha.2018.09.168.
[20] Daemi H, Barikani M. Synthesis and characterization of calcium alginate nanoparticles, sodium homopolymannuronate salt and its calcium nanoparticles. Sci Iran 2012;19:2023–8. https://doi.org/10.1016/j.scient.2012.10.005.
[21] Chan ES, Lee BB, Ravindra P, Poncelet D. Prediction models for shape and size of ca-alginate macrobeads produced through extrusion-dripping method. J Colloid Interface Sci 2009;338:63–72. https://doi.org/10.1016/j.jcis.2009.05.027.
[22] Hecht H, Srebnik S. Structural characterization of sodium alginate and calcium alginate. Biomacromolecules 2016;17:2160–7. https://doi.org/10.1021/acs.biomac.6b00378.
[23] Wang W, Naveed M, Baig MMFA, Abbas M, Xiaohui Z. Experimental rodent models of chronic prostatitis and evaluation criteria. Biomed Pharmacother 2018;108:1894–901. https://doi.org/10.1016/j.biopha.2018.10.010.
[24] Fonseca V, Schweizer A, Albrecht D, Baron MA, Chang I, Dejager S. Addition of vildagliptin to insulin improves glycaemic control in type 2 diabetes. Diabetologia 2007;50:1148–55. https://doi.org/10.1007/s00125-007-0633-0.
[25] Esposito K, Chiodini P, Maiorino MI, Capuano A, Cozzolino D, Petrizzo M, et al. A nomogram to estimate the hba1c response to different dpp-4 inhibitors in type 2 diabetes: a systematic review and meta-analysis of 98 trials with 24 163 patients. BMJ Open 2015:5. https://doi.org/10.1136/bmjopen-2014-005892.
[26] Scheen AJ. Dipeptidylpeptitase-4 inhibitors (Gliptins). Clin Pharmacokinet 2010;49:573–88. https://doi.org/10.2165/11532980-000000000-00000.
[27] Le XC, Kang D-K, Zhao W, Ali MM, Zhang Z, Ankrum JA, et al. Rolling circle amplification: a versatile tool for chemical biology, materials science and medicine. Chem Soc Rev 2014;43:3324. https://doi.org/10.1039/c3cs60439j.
[28] Matsumoto A, Kajiya H, Yamamoto-M N, Yanagi T, Imamura A, Okabe K, et al. Degradation rate of DNA scaffolds and bone regeneration. J Biomed Mater Res B Appl Biomater 2019;107:122–8. https://doi.org/10.1002/jbm.b.34102.
[29] Jiang Z, Shan K, Song J, Liu J, Rajendran S, Pugazhendhi A, et al. Toxic effects of magnetic nanoparticles on normal cells and organs. Life Sci 2019;220:156–61. https://doi.org/10.1016/j.lfs.2019.01.056.
[30] Seeliger MA, Maianti JP, Du XQ, Charron MJ, Leissring MA, Kleiner RE, et al. Anti-diabetic activity of insulin-degrading enzyme inhibitors mediated by multiple hormones. Nature 2014;511:94–8. https://doi.org/10.1038/nature13297.
[31] Storrie H, Mooney DJ. Sustained delivery of plasmid DNA from polymeric scaffolds for tissue engineering. Adv Drug Deliv Rev 2006;58:500–14. https://doi.org/10.1016/j.addr.2006.03.004.